Published in final edited form as:
Inflamm Bowel Dis. 2010 September ; 16(9): 1458–1466. doi:10.1002/ibd.21231.

Detection of Intestinal Inflammation by MicroPET Imaging Using a ^{64}Cu-Labeled Anti-β_7 Integrin Antibody

Jason LJ Dearling, PhD[1,2,*], **Eun Jeong Park, PhD**[2,3], **Patricia Dunning, BS**[1], **Amanda Baker, BS**[1], **Frederic Fahey, DSc**[1,2], **S Ted Treves, MD**[1,2], **Sulpicio G Soriano, MD**[2,3,4], **Motomu Shimaoka, PhD**[2,3], **Alan B Packard, PhD**[1,2], and **Dan Peer, PhD**[5,*]

[1] Division of Nuclear Medicine, Department of Radiology, Children's Hospital, Boston, 300 Longwood Avenue, Boston, MA 02115

[2] Harvard Medical School, 25 Shattuck Street, Boston, MA 02115

[3] Immune Disease Institute, 3 Blackfan Circle, The Center for Life Science Boston, Boston, MA 02115

[4] Department of Anesthesiology, Perioperative and Pain Medicine, Children's Hospital, Boston

[5] Laboratory of Nanomedicine, Department of Cell Research & Immunology, George S. Wise Faculty of Life Sciences, and the Center for Nanoscience and Nanotechnology Tel Aviv University, Tel Aviv 69978, Israel

Abstract

Background—The primary function of integrin β_7 is the recruitment and retention of lymphocytes to the inflamed gut. The aim of this study was to investigate the possibility of imaging colitis radioimmunodetection by targeting the β_7 integrin with a radiolabeled antibody.

Methods—FIB504.64, a monoclonal antibody which binds to β_7 integrin, was conjugated with a bifunctional chelator and labeled with ^{64}Cu. The antibody (50 μg, 7 MBq) was injected into C57BL/6 mice with experimentally induced colitis (n = 6). MicroPET images were collected at 1, 24, and 48 hours post-injection, and the biodistribution was measured at 48 hours by tissue assay. Data were also obtained for a ^{64}Cu-labeled non-specific isotype-matched antibody in mice with colitis, and ^{64}Cu-labeled FIB504 in healthy mice (n = 5 − 6).

Results—The microPET images showed higher uptake of ^{64}Cu-labeled FIB504 in the gut of mice with colitis than for either of the controls. This observation was confirmed by the 48 hour *ex vivo* biodistribution data: percentage of injected dose per gram of tissue (%ID/g ± SD) (large intestine) colitis mice with ^{64}Cu-labeled FIB504, 6.49 ± 2.25; control mice with ^{64}Cu-labeled FIB504, 3.64 ± 1.12; colitis mice, ^{64}Cu-labeled non-specific antibody 3.97 ± 0.48 %ID/g (p <0.05 between groups).

Conclusions—The selective uptake of ^{64}Cu-labeled FIB504 antibody in the gut of animals with colitis suggests that integrin β_7 may be a promising target for radioimmunodetection of this disease, which would aid diagnosis, assessment and therapy guidance of this disease.

Keywords

colitis; inflammatory bowel disease; radioimmunodetection; integrin targeting; copper-64

[*] Corresponding authors: JLJD, jason.dearling@childrens.harvard.edu, Division of Nuclear Medicine, Department of Radiology, Children's Hospital, Boston, 300 Longwood Ave., Boston, MA 02115., Tel: 001-617-919-2106, Fax: 001-617-730-0619; DP, peer@post.tau.ac.il, Laboratory of Nanomedicine, Department of Cell Research & Immunology, George S. Wise Faculty of Life Sciences, and the Center for Nanoscience and Nanotechnology, Tel Aviv University, Tel Aviv 69978, Israel, Tel: (972)-3-6407925, Fax: (972)-3-6405926.

Introduction

Inflammatory bowel disease (IBD), including ulcerative colitis and Crohn's disease, is an immune-mediated intestinal inflammation affecting 0.5-1% of the Western world's population [1]. This is a highly debilitating disease, which can have a severe impact on quality of life. As this is a chronic condition, treatment aims to keep it in remission by using anti-inflammatory and immunosuppressant drugs, with surgery required for more serious cases [2]. Clinical diagnosis of the severity of intestinal inflammation is important but remains to be established. Imaging would provide more global information, which could improve therapy, but currently routine practice is limited to ultrasound, X-ray, CT or MRI, which lack specificity. Currently there are potentially a number of methods of imaging intestinal inflammation (for review see [3] and [4]). Some are based on perturbations in metabolism and physiological effects, such as [^{18}F]FDG/PET which shows higher uptake in regions of tissue inflammation. However, there are a number of reasons why [^{18}F]FDG uptake can vary in the healthy bowel [5], [6]. Other techniques use single photon emission radionuclide imaging to detect non-specific antibody, or use autologous leukocytes, in both cases radiolabeled with either ^{99m}Tc or ^{111}In. The labeled leukocytes concentrate in regions of inflammation, and this method is often considered to be the gold standard for inflammatory imaging. This approach, however, requires that the technologists isolate the leukocytes, radiolabel them with ^{99m}Tc or ^{111}In, and then re-inject them, increasing the exposure of health workers to patient blood and also increasing the possibility that the blood cells will be contaminated during the labeling process. Antibodies raised against Non-specific Cross-reactive Antigen (NCA) and labeled with ^{99m}Tc [7], a molecule expressed on lymphocytes, have also been investigated. Evaluation of the condition is often made through invasive techniques, such as colonoscopy, which can only assess part of the intestine, and therefore give an incomplete indication of the extent of disease. In addition, this is an evaluation which is operator-dependent and lacks objectivity [8]. An objective method for the detection and description of intestinal inflammation is clearly needed, and medical imaging, such as Positron Emission Tomography (PET), is a potential way of solving this clinical problem.

These latter methods using labeled leukocytes focus on the basis of the pathology of this disease: chronic immune dysregulation is the primary cause of the inflammation and ulceration of the intestinal mucosa which form the pathology of the disease. This is mediated by the infiltration of leukocytes, and the β_7 positive leukocyte subset therefore present as a favorable target for an imaging agent, as they are both populous and a functional indicator of the location and degree of inflammation. The monomer β_7 is expressed on lymphocytes which have been activated in intestinal inductive sites, including Peyer's patches and mesenteric lymph nodes [9]. It is expressed as part of a heterodimeric integrin molecule in combination with either α_4 or α_E, the two resulting heterodimers being involved in recruitment and retention of lymphocytes to the inflamed intestine, respectively [10]. The $\alpha_4\beta_7$ integrin binds to mucosal addressin cell-adhesion molecule-1 (MAdCAM-1) which is constitutively expressed on endothelial cells in the intestine [10]. The $\alpha_E\beta_7$ integrin is expressed by lymphocytes in mucosal epithelial sites and is involved in lymphocyte binding to E-cadherin, resulting in retention. The β_7 integrin represents a promising target for detection of colitis because of its specificity of expression by lymphocytes in this organ, being involved only in lymphocyte recruitment to the inflamed gut and not to other principal organs such as lung or liver [11].

Our aim in this study was to investigate whether the antibody FIB504 would have increased uptake in the intestines of mice with colitis. The antibody was radiolabeled with the positron-emitting radionuclide ^{64}Cu and injected into mice with experimental colitis induced

by dextran sodium sulphate (DSS) [12], [13], [14], [15]. ^{64}Cu was chosen because its half-life is commensurate with antibody pharmacokinetics. MicroPET imaging was used in combination with *ex vivo* tissue assay to measure radionuclide distribution in this acute model of colitis to investigate whether there was specific uptake in the inflamed gut.

Materials and Methods

General

Chemicals and reagents were obtained from Sigma-Aldrich unless otherwise specified. EDC (1-ethyl-3-(3-(dimethylamino)propyl)carbodiimide hydrochloride) was purchased from Pierce (Rockford IL, USA). *S*-2-(4-aminobenzyl)-1,4,7,10-tetraazacyclododocane tetraacetic acid (NH_2-*p*-Bn-DOTA) was purchased from Macrocyclics (Dallas, TX). Metal-naive pipette tips were purchased from Rainin (Oakland, CA). Glass and plasticware were washed with 10% HNO_3 and rinsed thoroughly with ultrapure water (> 15 MΩ resistivity) (Millipore, Billerica, MA) before use. Ultrapure water was also used in buffer preparation. Sodium acetate buffer (0.1 M, pH 5.0) was used for conjugation and radiolabeling. Metal contaminants in the buffer were decreased by passing through a Chelex-100 resin column (Bio-Rad Laboratories, Hercules, CA).

Antibody-chelator conjugation

The anti-β_7 antibody was produced from its hybridoma (FIB504.64 [16]) and was purified using a HiTrap Protein G column (GE Healthcare; Piscataway, NJ). The control antibody was Rat IgG2a (BD Biosciences; San Jose, California).

The antibody was buffer exchanged into sodium acetate (0.1 M, pH 5.0) and concentrated to approximately 10 mg/mL using spin column filters (Centricon, Millipore, Bedford MA) (MWCO 30 kDa). The bifunctional chelator NH_2-*p*-Bn-DOTA was conjugated to the antibody using previously described methods [17]. Briefly, to NH_2-*p*-Bn-DOTA in Me_2SO (25 mg/mL) was added 3 volume equivalents of 0.1 M sodium acetate buffer (pH 5.0) to give a final bifunctional chelator concentration of approximately 100 mg/mL. The pH was brought to 5.0 by addition of NaOH. The chelator was added to the antibody at a molar ratio of 250:1, followed by buffer, and then 500 molar equivalents of EDC, which was made up immediately before use in ultrapure water at a concentration of 50 mg/mL. The volume of reagents added diluted the antibody to a final concentration of 5 mg/mL. The reaction was gently mixed by pipetting, centrifuged to remove air bubbles, pH was confirmed to be 5.0, and then the reaction was placed in a 37°C water bath. The final concentration of Me_2SO was always < 5% (typically ~ 1%). After 30 minutes unbound chelator was separated from the immunoconjugate by size exclusion HPLC (BioSep SEC-S3000 column; Phenomenex, Torrance, CA) with an isocratic aqueous phase of 0.1 M sodium acetate, pH 5.0. Retention time of the immunoconjugate was typically 8.1 minutes, with the unbound chelator eluting at approximately 11.0 minutes. Purified immunoconjugate fractions were pooled, concentrated, and then stored in aliquots at -80 °C.

Immunoreactivity assay

The immunoreactivity of the BFC-conjugated antibody was assayed by flow cytometry [18]. Briefly, 10^6 TK-1 cells (Mouse T cells lymphoma) expressing $\alpha_4\beta_7$ integrin was stained with 10 μg/mL purified FIB504.64 or with the immunoconjugate for 30 minutes at 4 °C. Then, the cells were washed twice with FACS buffer (PBS + 2% Fetal Calf Serum) and counter stained with 2nd mAb against rat IgG2a – Alexa 488 conjugate at 4 °C for 30 min and subjected to flow cytometry (FACScan, BD Biosciences, San Jose, CA).

Isotope dilution assay

Ratio of protein molecules to available chelating molecules was measured using similar methods to those reported by Meares *et al*. [19]. Typically, a solution of immunoconjugate of known concentration (approx. 3 mg/mL) was prepared. A small amount of ^{64}Cu was added to a solution of cold copper prepared from a commercially available standard (Sigma Aldrich, St Louis MO) the concentration of which was approximately twice the estimated concentration of available chelators on the antibody. This solution was vortexed, centrifuged, and left for at least 1 h at room temperature. To 10 μL of NaOAc buffer in an Eppendorf micro centrifuge tube was added 10 μL of the cold copper/^{64}Cu mixture, followed by 10 μL of the antibody. The reaction was then mixed by pipetting and incubated at room temperature for at least 1 hour. Then 1 μL of the labeled protein was removed and added to 9 μL phosphate buffer (0.1 M, pH 8) containing 100 mM ethylenediamine-tetraacetic acid (EDTA). After 5 minutes 1 μL of the solution was spotted onto an ITLC plate (Instant Thin-Layer Chromatography Si Gel impregnated glass fiber sheets; Pall Life Sciences, Ann Arbor, MI), which was allowed to air dry and then developed using phosphate buffer (0.1 M, pH 8, 100 mM EDTA) as the mobile phase. The plate was cut into four sections and radioactivity in the sections was assayed using a gamma counter. Using these conditions, labeled antibody remains at the baseline of the plate with free copper moving with the solvent front. TLCs were also run of antibody incubated with no cold copper, 10 mM cold copper (to block all binding sites) and concentrations of copper lower than and higher than the target concentration. The number of available binding sites was calculated by the method reported [19].

Radiolabeling

For imaging studies immunoconjugates were radiolabeled with ^{64}Cu as previously described. For example, to 2 mCi ^{64}Cu in 5-10 μL HCl (0.04 N) was added approximately 3 volume equivalents of pH 5, 0.1 M acetate buffer. To this was added the antibody (e.g. 250 μg, 75 μL), also in acetate buffer. After 30 min. incubation at 25°C 1 μL of the reaction mixture was removed and added to 9 μL phosphate buffer (0.1 M, pH 8) containing 100 mM EDTA. A TLC was run as before to assess radiolabeling (>95% required for injection). The radioimmunoconjugate was diluted with saline and sterile filtered (0.2 μm) before injection.

Experimental colitis model

Dextran sodium sulphate (DSS, 36-50 kDa MW, from MP Biomedicals, Solon, OH), which is known to induce inflammation throughout the bowel [12], [13], [14], [15], was included in the drinking water for 8 days at 2.0 % (w/v).

Biodistribution studies

Three groups of mice were involved in this study, one test group and two control groups: Group 1 (n = 6) was treated with DSS and injected with the radiolabeled anti-β7 antibody; Group 2 (n = 5) was not treated with DSS and was injected with the radiolabeled specific anti-β7 antibody; and Group 3 (n = 5) was treated with DSS and injected with a ^{64}Cu-labeled non-specific isotype-matched antibody (Rat IgG_{2a}). After 9 days of DSS treatment the radiolabeled antibody was injected into the tail vein of the mice (50 μg protein, 7.1 ± 1.2 (mean ± SD) MBq, 0.1 mL in saline). MicroPET images were collected for 30 min. using a Siemens Focus 120 camera at 1, 24 and 48 h post injection. At 48 h post-injection, microCT images were also collected using a Siemens MicroCAT II camera. After the microCT images were obtained at 48 h post-injection, the mice were euthanized by CO_2 inhalation, and an *ex vivo* tissue biodistribution was carried out. Tissues were collected, weighed and radioactivity was assayed using a Packard Cobra II automated gamma counter (Meriden, CT). MicroPET and microCT images were registered manually using AMIDE software (A

Medical Imaging Data Examiner, http://amide.sourceforge.net/index.html). Data from volumes of interest (VOIs) within relevant tissues were used to calculate biodistribution throughout the imaging study.

Statistical analysis

Statistical analysis was carried out using SPSS V 14.0 for Windows. The 48 h post-injection *ex vivo* biodistribution data was analyzed for statistical significance by ANOVA, with *post hoc* analysis adjusted using the Bonferroni correction. Differences were considered significant at the 5 % level ($p < 0.05$).

Results

DSS model

Including DSS in the drinking water resulted in body weight loss, as is shown for treated and control groups in Figure 1. Mean decrease in total body weight was 5.43 ± 7.13 % for treated mice; body weight gain for non-treated mice was 5.9 ± 0.75 % over the same period. In our experience, this pattern of initial increase and then decrease in body weight is typical for mice treated with this level of DSS (2 % w/v) [12]. For all DSS-treated mice feces became more liquid during the course of the study and hemorrhage from the bowel was observed at necropsy.

Immunoreactivity assay

In order to determine whether the conjugation of the chelator reduced the binding capacity of the anti-β_7 integrin mAb (FIB504.64) to its target, we examined the binding of FIB504.64 to TK-1 model cells. Flow cytometry data (Figure 2) indicated that the immunoreactivity of the antibody was not impaired by the conjugation of the bifunctional chelator.

Isotope dilution assay and antibody radiolabeling

The number of chelators per protein was 1.06 ± 0.14 for the non-specific control antibody and 1.05 ± 0.09 for FIB504 (mean of three separate determinations ± SD). The antibodies labeled at specific activities of between 194: 1 and 296: 1 (MBq: mg) and radiochemical purity was always > 95 % before injection.

Blood pharmacokinetics of the radiolabeled antibodies

At 1, 24 and 48 h post-injection (p.i.), blood was taken by tail vein nick and radioactivity assayed. The results are presented in Figure 3. As the inflamed intestine of group 1 showed higher uptake of the specific antibody it could be that the lower blood radioactivity is due to sequestration in the gut of group 1, while in group 3 the non-specific antibody had no target organ or tissue, resulting in a longer blood half-life. There was a statistical difference ($p < 0.05$) in the radioactivity in the blood between groups 1 (test group) and 3 (control group, non-specific antibody, DSS treated mice) at both 24 and 48 h with activity in group 1 lower at both time points (group 1; 12.93 ± 2.12 percentage of injected dose per gram of tissue (%ID/g), 7.29 ± 3.29 %ID/g: group 2; 20.63 ± 3.69, 12.62 ± 1.33: means ± SD at 24 and 48 hours, respectively).

MicroPET Imaging

Representative microPET images are shown in Figure 4. The distribution of radionuclide at 1, 24 and 48 h p.i. in DSS-treated mice injected with the ^{64}Cu-labeled anti-β_7 antibody are shown in Figures 4A (1-3). The images show that the radiolabeled antibody was initially (at 1 hour p.i.) distributed throughout the blood pool with some activity in the bladder, that by 24 h p.i. there was some specific uptake in the target area, and that by 48 h p.i. the

radionuclide was clearing from the blood and that there was specific uptake in the gut. For comparison microPET/microCT images of radionuclide distributions in control mice at 48 h p.i. (Figures 4B and 4C) show similar radionuclide levels in the normal organs but much lower levels in gut for non-DSS-treated mice injected with the radiolabeled specific antibody (Figure 4B), and for DSS-treated mice injected with radiolabeled isotype-matched non-specific antibody (Figure 4C).

Values from volumes of interest (VOI) drawn around organs were converted to %ID/g ± estimate of the standard deviation (ESD) and are presented as bar graphs in Figure 5. Patterns of clearance from non-target tissues are typical for a radiolabeled antibody. High initial uptake in the liver shows evidence of clearing by 48 h, as does radioactivity in the kidney. Radioactivity is clearing more rapidly from the lung following blood clearance. Muscle and brain have very low levels of radionuclide, which clear from these tissues throughout the study. Radioactivity levels in the gut were relatively stable throughout the time course studied for all groups. While there was higher uptake of antibody in the gut in group 1 (5.47 ± 2.0), it was not as different from the other groups as in the *ex vivo* dissection biodistribution (%ID/g ± ESD by image analysis in the gut for group 2 was 4.44 ± 1.2, for group 3 was 4.24 ± 0.14). This reflects the difficulty in identifying large intestine in the image. These data are also not a fair reflection of the variation of antibody uptake within the gut. As can be seen in Figure 4 there are a number of hot spots of high uptake of radionuclide in the gut of group 1 which are not seen in the other groups. For example, the 90th percentile values of the gut VOIs from the individuals in the images for groups 1, 2 and 3 were 14.23 %ID/g, 5.02 %ID/g and 7.48 %ID/g, respectively. To represent the range of counts in the gut VOIs the %ID/g for each voxel was calculated for a mouse from each of the three groups. These data are presented in Figure 5 as line graphs. It can be seen that the count distributions for control groups 2 and 3 follow an approximation to a normal distribution about the mean at all time points. However, the graphs for group 1 have a much more heterogeneous distribution with much higher maximal uptake values due to these hot spots. This is evident at both 24 and 48 h p.i.

Ex vivo biodistribution assay

The results of the 48 hour post injection *ex vivo* biodistribution assay and the results from statistical analysis of this data are given in Table 1. Uptake in the large intestine was higher for the test group than for the controls, achieving statistical significance between groups 1 and 2 (%ID/g in large intestine: group 1 = 6.49, group 2 = 3.64, group 3 = 3.97). The lack of differential between the groups for stomach and small intestine is surprising, as DSS causes inflammation throughout the digestive tract. However, it has been reported that DSS has a greater effect on the large intestine than the rest of the gut [13].

The lower amount of radioactivity in blood, heart, lung and kidney for group 1 compared with the other two groups might have been due to sequestration in the large intestine. The differences in antibody uptake in liver and spleen could have a biological basis rather than be due to clearance because the specific antibody had higher uptake in these organs in control mice compared with DSS-treated mice, and also uptake of non-specific antibody in DSS-treated mice was lower in these organs (%ID/g for liver: group 1 = 8.48, group 2 = 11.57, group 3 = 6.72). Uptake of the specific antibody in liver in DSS-treated mice might have been restricted by uptake in the target organ.

Discussion

The development of an imaging agent specific for colonic inflammation would aid in its diagnosis, assessment and in evaluating response to therapy. It is important to have a measure of not only the existence, but also the degree of disease. The presence of white

blood cells is a reliable indicator of inflammation, though infection also has to be taken into account. In this study, we report the biodistribution of antibody FIB504 that binds to the integrin β_7, which is expressed mainly on gut lymphocytes. This integrin, in combination with integrins α_4 and α_E, plays a role in the recruitment to and retention of lymphocytes in the intestine. Higher uptake of the radiolabeled antibody in the intestine of mice with acute colitis compared with controls was found by both microPET imaging and *ex vivo* tissue assay, suggesting that the β_7 integrin monomer could be a viable target for colitis imaging and that the radiolabeled antibody, targeting a subset of lymphocytes, could serve as a specific imaging agent. It is difficult to comment on which integrin heterodimer, $\alpha_4\beta_7$ or $\alpha_E\beta7$, is the major target for this antibody *in vivo*. This could be investigated in future work comparing, for example, the biodistribution data obtained in this study (FIB504) and DATK32 which binds to $\alpha_4\beta_7$ [16].

Previous work in developing imaging agents for nuclear medicine has focused on the distribution of white blood cells (lymphocytes, macrophages and neutrophils, which have been detected through either *ex vivo* or *in vivo* radiolabeling. There has been an almost chronological increase in the specificity of agents used for inflammation imaging. Gallium-67 concentrates at sites of infection, possibly through more than one mechanism: uptake of the metal into circulating leukocytes which then concentrate at the infected area, by the infectious agents themselves via siderophores, or by concentration at the site of infection by binding to lactoferrin excreted by leukocytes, might all play a role [20]. Non-specific radiolabeled IgG also shows uptake in inflamed tissue, with the Fc region being necessary for concentration [21]. Liposomes have also been used for inflammation imaging, concentration in inflamed tissues being due to non-specific uptake [22]. More targeted methods focus on imaging lymphocytes by either autologous reintroduction of radiolabeled leukocytes, or through *in vivo* labeling methods, such as the injection of an antibody that binds to granulocytes. The murine IgG1 antigranulocyte antibody BW250/183 binds to the non-specific cross-reacting antigen (NCA-95) which is expressed on granulocytes [23], but it is also expressed on normal gut mucosa, challenging specificity of the technique [24]. In a comparison of non-specific IgG, liposomes and granulocytes it was found that all visualized colonic inflammation within 1 h [25]. Neutrophil binding ^{99m}Tc-labeled IL-8 was found to give similar uptake in inflamed gut as ^{99m}Tc-HMPAO-labeled leukocytes at 1 h, but radiolabeled IL-8 uptake continued to increase in diseased gut up to 4 h, enabling better discrimination of inflamed regions of tissue [26]. Kanwar *et al.* [27] reported that localization of ^{111}In-labeled anti-CD4$^+$ antibody to DSS-inflamed gut correlated well with pathology. More closely related to this work is the use of anti-MAdCAM-1 antibody (MECA-367) to functionalize microbubbles for ultrasound detection of colitis [28]. Again, there was a strong correlation between uptake and pathological inflammatory scores.

Targeting leukocytes does have some disadvantages. For example, they can make their way through the diseased bowel wall and into the stool, so regions of bowel distal to the disease site are visualized, depending on when the imaging takes place in relation to the injection of radiolabeled material. Serial imaging can overcome this obstacle, as can use of a high resolution imaging technique, such as PET, in order to discriminate intraluminal residence of the radionuclide from that in the intestine. Uptake at the target site will have been raised by the increased permeability at sites of inflammation, although this might also have increased non-specific accumulation of radiolabeled antibody. The presence of macrophages at sites of colonic inflammation might also increase non-specific accumulation of this whole antibody through interaction with the Fcγ receptors of invading neutrophils and macrophages.

It is relevant to note that antibodies binding to these molecules can be employed therapeutically. Patients treated with anti-$\alpha_4\beta_7$ antibody (MLN02) had a higher probability

of clinical remission within 6 weeks than a placebo-treated control group ($p = 0.03$) [29]. This might have relevance to this study because 50 μg of radiolabeled antibody was given to each mouse, which for a 25 g mouse means that the antibody was given at 2.0 mg/kg, which was the highest level given to the patients with therapeutic effect. Therefore the radiolabeled antibody could have effected the lymphocyte trafficking. Future studies could investigate the effects of varying the amounts of administered antibody on the imaging and distribution data.

In this study, an acute experimental murine model of colitis has been employed. As with all animal models, this model has advantages and potential shortfalls. It has been reported that DSS can bind directly to the β_7 integrin [30]. This could have perturbed the study in two ways: antibody binding of β_7 could have been decreased through physical blocking by DSS; or expression of β_7 by the lymphocytes could have been up regulated to compensate for DSS binding. In future studies other models will be investigated which do not involve DSS and are more relevant to the chronic clinical situation. For example, adoptive T transfer is a more chronic model simulating the prolonged inflammation typical of Crohn's disease and ulcerative colitis [31], and T-bet deficient mice that spontaneously develop colitis would be more similar to ulcerative colitis disease [32].

Data has so far been collected at the macro scale, but to fully understand the images obtained, higher resolution data are needed. Therefore, autoradiography will also be employed to study the localization of radionuclide in relation to histopathologically demonstrated tissue inflammation, Peyer's patches, mesenteric lymph nodes, and other relevant tissues.

Conclusion

In this report, we describe the radiolabeling of an anti-β_7 integrin antibody and its use in detecting acute colitis in an experimental murine model using microPET.

Use of β_7 monomer as a target for colitis imaging not only identifies a new target, but also introduces a more specific level of inflammation targeting. The lymphocytes expressing β_7 are not only in regions of inflamed gut, but they have been locally activated as a result of the inflammation.

Further work in this area will focus on two main areas. First, the molecular properties of the targeting agent will be manipulated to improve its characteristics as an imaging agent, by for example reducing its molecular weight which will shorten its blood half-life and accelerate clearance from non-target organs. Second, the targeting ability of the antibody will be employed to develop specific delivery systems for therapy of the colonic inflammation [18].

Acknowledgments

We gratefully acknowledge support from the CHMC Anesthesia Foundation (to S.G.S.), and the National Institutes of Health, AI063421 and HL048675 (M.S.), Alon Foundation and the IRG-FP7 of the European Union (D.P.). Copper-64 was produced at Washington University School of Medicine (St Louis MO), under the support of National Cancer Institute Grant R24CA86307.

Research Support: CHMC Anesthesia Foundation (S.G.S.), National Institutes of Health, AI063421 and HL048675 (M.S.), Alon Foundation and IRG-FP7, European Union (D.P.).

References

1. Loftus EV Jr, Sandborn WJ. Epidemiology of inflammatory bowel disease. Gastroenterol Clin North Am. 2002; 31:1–20. [PubMed: 12122726]

2. Baumgart DC, Sandborn WJ. Inflammatory bowel disease: clinical aspects and established and evolving therapies. Lancet. 2007; 369:1641–57. [PubMed: 17499606]
3. Gyorke T, Duffek L, Bartfai K, et al. The role of nuclear medicine in inflammatory bowel disease. A review with experiences of aspecific bowel activity using immunoscintigraphy with ^{99m}Tc anti-granulocyte antibodies. Eur J Radiol. 2000; 35:183–92. [PubMed: 11000561]
4. Basu S, Zhuang H, Torigian DA, et al. Functional imaging of inflammatory diseases using nuclear medicine techniques. Semin Nucl Med. 2009; 39:124–45. [PubMed: 19187805]
5. Miraldi F, Vesselle H, Faulhaber PF, et al. Elimination of artifactual accumulation of FDG in PET imaging of colorectal cancer. Clin Nucl Med. 1998; 23:3–7. [PubMed: 9442955]
6. Shreve PD, Anzai Y, Wahl RL. Pitfalls in oncologic diagnosis with FDG PET imaging: physiologic and benign variants. Radiographics. 1999; 19:61–77. quiz 150-1. [PubMed: 9925392]
7. Ivancevic V, Wolter A, Munz DL. Nonspecific bowel activity in imaging inflammation with Tc-99m labelled monoclonal anti-NCA-90 Fab' fragment MN3. Nuklearmedizin. 2001; 40:71–4. [PubMed: 11475075]
8. Baron JH, Connell AM, Lennard-Jones JE. Variation between Observers in Describing Mucosal Appearances in Proctocolitis. Br Med J. 1964; 1:89–92. [PubMed: 14075156]
9. Johansson-Lindbom B, Agace WW. Generation of gut-homing T cells and their localization to the small intestinal mucosa. Immunol Rev. 2007; 215:226–42. [PubMed: 17291292]
10. Shaw SK, Brenner MB. The beta 7 integrins in mucosal homing and retention. Semin Immunol. 1995; 7:335–42. [PubMed: 8580465]
11. Hamann A, Andrew DP, Jablonski-Westrich D, et al. Role of alpha 4-integrins in lymphocyte homing to mucosal tissues in vivo. J Immunol. 1994; 152:3282–93. [PubMed: 7511642]
12. Park EJ, Takahashi I, Ikeda J, et al. Clonal expansion of double-positive intraepithelial lymphocytes by MHC class I-related chain A expressed in mouse small intestinal epithelium. J Immunol. 2003; 171:4131–9. [PubMed: 14530335]
13. Kullmann F, Messmann H, Alt M, et al. Clinical and histopathological features of dextran sulfate sodium induced acute and chronic colitis associated with dysplasia in rats. Int J Colorectal Dis. 2001; 16:238–46. [PubMed: 11515684]
14. Cooper HS, Murthy SN, Shah RS, et al. Clinicopathologic study of dextran sulfate sodium experimental murine colitis. Lab Invest. 1993; 69:238–49. [PubMed: 8350599]
15. Okayasu I, Hatakeyama S, Yamada M, et al. A novel method in the induction of reliable experimental acute and chronic ulcerative colitis in mice. Gastroenterology. 1990; 98:694–702. [PubMed: 1688816]
16. Andrew DP, Berlin C, Honda S, et al. Distinct but overlapping epitopes are involved in alpha 4 beta 7-mediated adhesion to vascular cell adhesion molecule-1, mucosal addressin-1, fibronectin, and lymphocyte aggregation. J Immunol. 1994; 153:3847–61. [PubMed: 7523506]
17. Di Bartolo N, Sargeson AM, Smith SV. New ^{64}Cu PET imaging agents for personalised medicine and drug development using the hexa-aza cage, SarAr. Org Biomol Chem. 2006; 4:3350–7. [PubMed: 17036125]
18. Peer D, Park EJ, Morishita Y, et al. Systemic leukocyte-directed siRNA delivery revealing cyclin D1 as an anti-inflammatory target. Science. 2008; 319:627–30. [PubMed: 18239128]
19. Meares CF, McCall MJ, Reardan DT, et al. Conjugation of antibodies with bifunctional chelating agents: isothiocyanate and bromoacetamide reagents, methods of analysis, and subsequent addition of metal ions. Anal Biochem. 1984; 142:68–78. [PubMed: 6440451]
20. Palestro CJ. The current role of gallium imaging in infection. Semin Nucl Med. 1994; 24:128–41. [PubMed: 8023169]
21. Rubin RH, Fischman AJ, Callahan RJ, et al. ^{111}In-labeled nonspecific immunoglobulin scanning in the detection of focal infection. N Engl J Med. 1989; 321:935–40. [PubMed: 2779615]
22. Awasthi V, Goins B, McManus L, et al. [^{99m}Tc] liposomes for localizing experimental colitis in a rabbit model. Nucl Med Biol. 2003; 30:159–68. [PubMed: 12623115]
23. Burtin P, Quan PC, Sabine MC. Nonspecific cross reacting antigen as a marker for human polymorphs, macrophages and monocytes. Nature. 1975; 255:714–6. [PubMed: 49025]

24. Bosslet K, Luben G, Schwarz A, et al. Immunohistochemical localization and molecular characteristics of three monoclonal antibody-defined epitopes detectable on carcinoembryonic antigen (CEA). Int J Cancer. 1985; 36:75–84. [PubMed: 2410375]
25. Dams ET, Oyen WJ, Boerman OC, et al. Technetium-99m-labeled liposomes to image experimental colitis in rabbits: comparison with technetium-99m-HMPAO-granulocytes and technetium-99m-HYNIC-IgG. J Nucl Med. 1998; 39:2172–8. [PubMed: 9867164]
26. Gratz S, Rennen HJ, Boerman OC, et al. Rapid imaging of experimental colitis with (99m)Tc-interleukin-8 in rabbits. J Nucl Med. 2001; 42:917–23. [PubMed: 11390557]
27. Kanwar B, Gao DW, Hwang AB, et al. In vivo imaging of mucosal CD4+ T cells using single photon emission computed tomography in a murine model of colitis. J Immunol Methods. 2008; 329:21–30. [PubMed: 17964595]
28. Bachmann C, Klibanov AL, Olson TS, et al. Targeting mucosal addressin cellular adhesion molecule (MAdCAM)-1 to noninvasively image experimental Crohn's disease. Gastroenterology. 2006; 130:8–16. [PubMed: 16401463]
29. Feagan BG, Greenberg GR, Wild G, et al. Treatment of ulcerative colitis with a humanized antibody to the alpha4beta7 integrin. N Engl J Med. 2005; 352:2499–507. [PubMed: 15958805]
30. Ni J, Chen SF, Hollander D. Effects of dextran sulphate sodium on intestinal epithelial cells and intestinal lymphocytes. Gut. 1996; 39:234–41. [PubMed: 8991862]
31. Park EJ, Mora JR, Carman CV, et al. Aberrant activation of integrin alpha4beta7 suppresses lymphocyte migration to the gut. J Clin Invest. 2007; 117:2526–38. [PubMed: 17786243]
32. Garrett WS, Lord GM, Punit S, et al. Communicable ulcerative colitis induced by T-bet deficiency in the innate immune system. Cell. 2007; 131:33–45. [PubMed: 17923086]

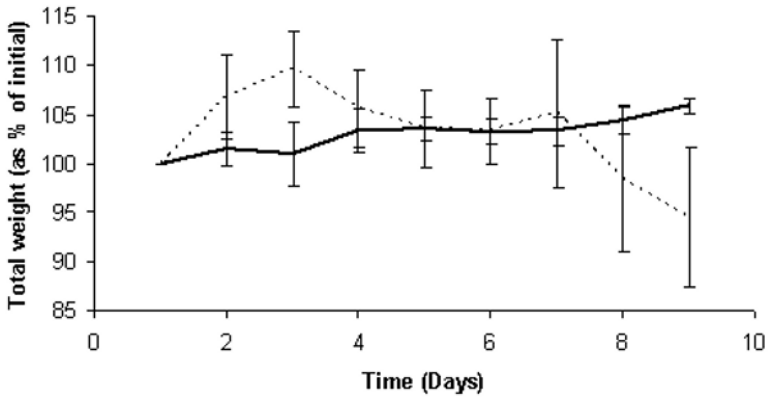

Figure 1. Bodyweight changes in mice treated with dextran sodium sulfate in order to experimentally induce colitis

Total body weights (means ± SD) of control (solid line) and DSS-treated mice (2 % w/v in water, dashed line). This pattern of increase and decrease is typical.

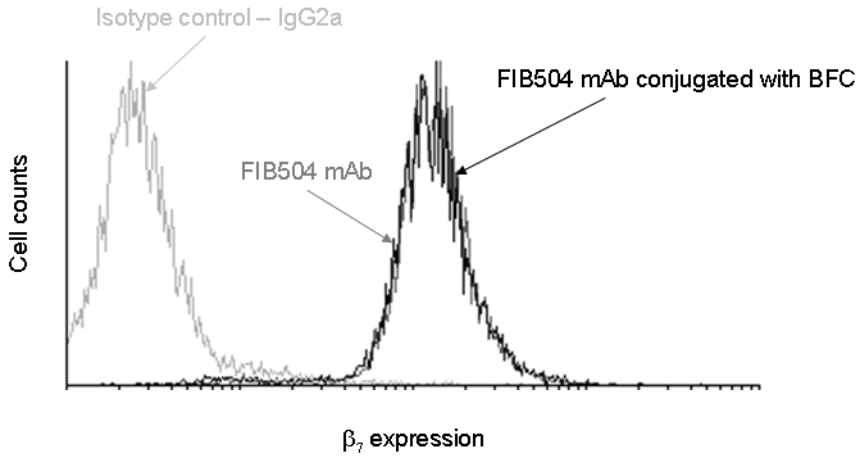

Figure 2. Conjugation of BiFunctional Chelator to FIB504.64 does not impair the binding of the antibody

A representative histogram confirming that the antigen binding of this anti-β_7 antibody was not impaired by conjugation with BFC NH_2-*p*-Bn-DOTA. Note that the data for pre-and post-conjugation antibody binding are almost superimposed.

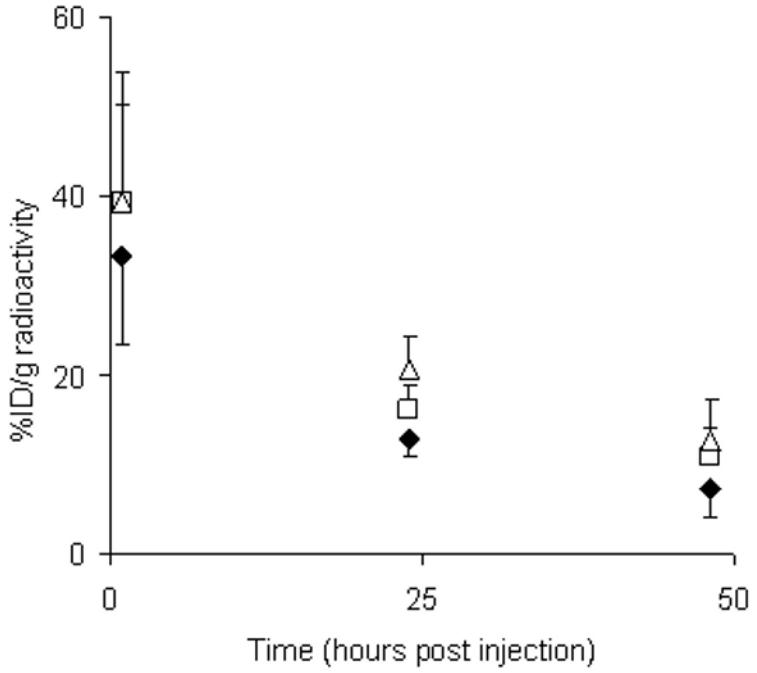

Figure 3. Blood pharmacokinetics of radiolabeled antibodies in DSS induced colitis mice

Pharmacokinetics (percentage of injected dose per gram of tissue, %ID/g) of radiolabeled antibodies in mouse blood at 1, 24 and 48 hours post injection. Diamonds = group 1 (test), squares = group 2 (control, specific antibody, no colitis), triangles = group 3 (control, non-specific antibody, colitis). The antibody cleared from the blood pool in a typical pattern for a whole antibody. Lower levels of radiolabeled antibody in the blood of the test group could be due to sequestration in the inflamed gut. The decay corrected data presented are the means ± SD for n = 5-6.

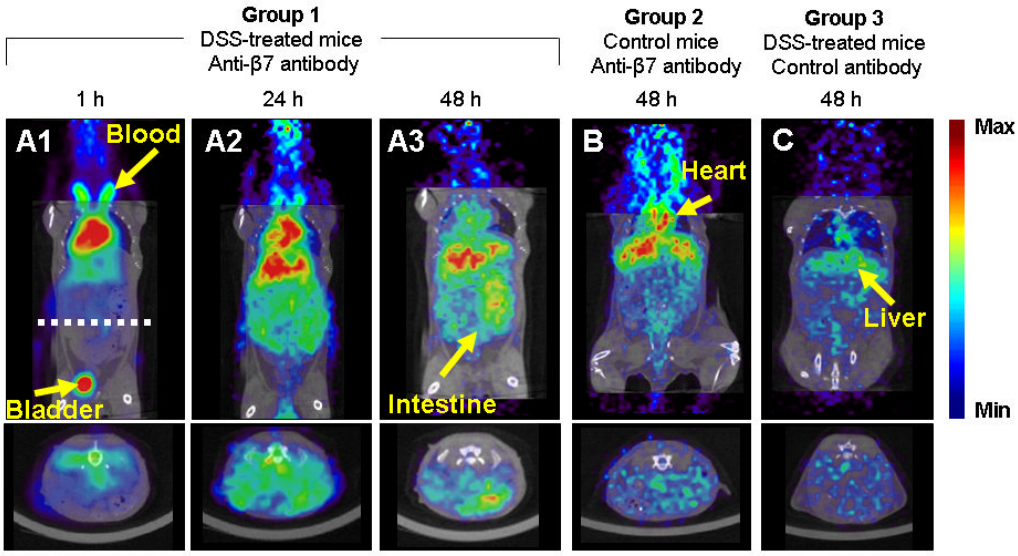

Figure 4. MicroPET biodistribution of ^{64}Cu anti-β_7 mAb in DSS-induced mice

Representative microPET images (color scale, microCT images for anatomic reference in grayscale) of the distribution of ^{64}Cu radionuclide following injection of the radiolabeled antibodies. Figures 4A-C are representative of images obtained from the test group at 1, 24 and 48 hours post-injection. Uptake of the radiolabeled anti-β_7 antibody in the inflamed gut is evident in the coronal (top panel) and transaxial images (bottom panel, taken at dashed white line in 4A). Radionuclide uptake in the gut was lower for control groups 2 and 3 (Figures 4B and C, respectively).

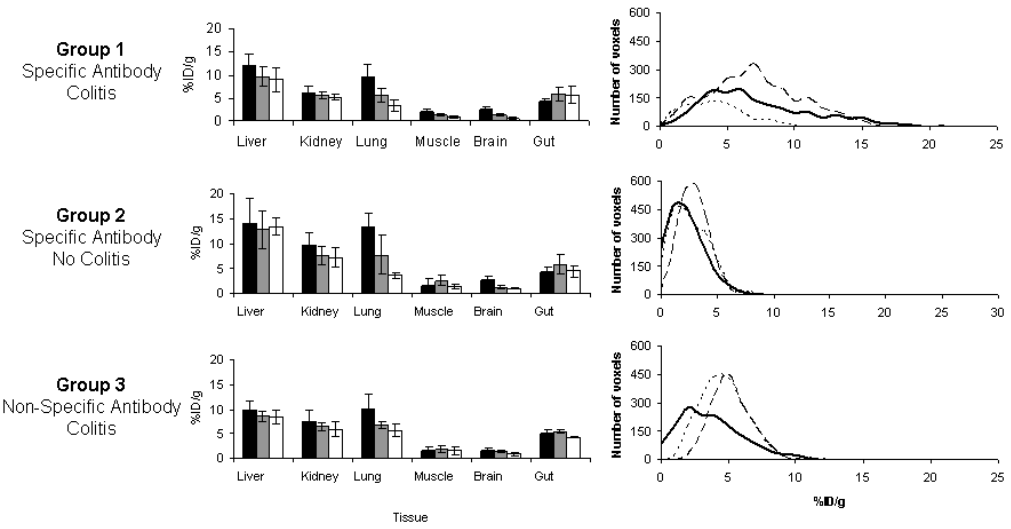

Figure 5. Analysis of biodistribution data obtained from microPET

Biodistribution data obtained from microPET images. Data obtained at 1 h (black), 24 h (gray) and 48 h (white) post injection of radiolabeled antibody. Volumes of interest (VOI) were drawn around organs and the counts were converted to %ID/g (± ESD). High uptake was found in the liver and kidneys. Radionuclide cleared from the lung following blood clearance, and was low in muscle and brain. A VOI was drawn around the gut resulting in averaging of high and low regions of uptake. Radioactivity concentration-frequency line graphs for VOIs for the gut regions of individuals at 1 h (dotted line), 24 h (dashed line) and 48 h post injection are presented, that give a better representation of foci of high uptake in the test group compared with controls.

Table 1

***Ex vivo* dissection biodistribution data for the three groups at 48 h post-injection**

Higher uptake of radiolabeled anti-β_7 integrin monomer antibody FIB504 was detected in the large intestine of mice treated with DSS compared with control groups 2 and 3. Data are percentage injected dose per gram (%ID/g) (mean ± SD). Statistical differences of $p < 0.05$ are highlighted in bold. The Bonferroni correction was used for *post hoc* analysis.

Tissue	Group 1 Colitis Specific Antibody	Group 2 No Colitis Specific Antibody	Group 3 Colitis Non-Specific Antibody	ANOVA Differences between groups	*Post hoc* analysis 1 vs 2	1 vs 3	2 vs 3
Blood	6.56 ± 2.46	10.91 ± 6.26	12.61 ± 1.35	0.056	0.258	0.068	1.000
Heart	1.91 ± 0.52	4.26 ± 1.37	3.91 ± 0.77	**0.002**	**0.003**	**0.011**	1.000
Lung	4.99 ± 1.63	7.49 ± 2.54	8.16 ± 1.21	**0.032**	0.136	**0.044**	1.000
Liver	8.48 ± 1.57	11.57 ± 2.01	6.72 ± 1.22	**0.001**	**0.023**	0.293	**0.001**
Spleen	6.58 ± 2.31	10.02 ± 3.86	2.79 ± 0.53	**0.003**	0.141	0.094	**0.002**
Kidney	3.94 ± 1.01	6.04 ± 1.80	5.28 ± 0.77	0.085	0.274	0.892	1.000
Stomach	1.93 ± 0.46	2.97 ± 2.08	2.19 ± 0.59	0.388	0.560	1.000	1.000
Small Intestine	3.83 ± 1.15	4.30 ± 1.61	2.78 ± 0.17	0.138	1.000	0.462	0.169
Large Intestine	6.49 ± 2.25	3.64 ± 1.12	3.97 ± 0.48	**0.024**	**0.038**	0.095	1.000
Brain	0.24 ± 0.05	0.41 ± 0.13	0.46 ± 0.12	**0.009**	0.062	**0.011**	1.000
Muscle	0.61 ± 0.20	1.31 ± 0.90	0.60 ± 0.14	0.072	0.125	1.000	0.144
Bone	1.24 ± 0.68	2.40 ± 1.29	0.86 ± 0.22	**0.031**	0.121	1.000	**0.037**
n =	6	5	5				